

Fractality of Hofstadter Butterfly in Specific Heat Oscillation

Li-Ping YANG^{1*}, Wen-Hu XU², Ming-Pu QIN³, and Tao XIANG^{3,4}

¹*Institute for Theoretical Solid State Physics, IFW-Dresden, 01069 Dresden, Germany*

²*Department of Physics and Astronomy, Rutgers University, Piscataway, NJ 08854, U.S.A.*

³*Institute of Physics, Chinese Academy of Sciences, P. O. Box 603, Beijing 100190, China*

⁴*Institute of Theoretical Physics, Chinese Academy of Sciences, P. O. Box 2735, Beijing 100190, China*

(Received December 26, 2011; accepted February 20, 2012; published online March 27, 2012)

We calculate thermodynamical properties of the Hofstadter model using a recently developed quantum transfer matrix method. We find intrinsic oscillation features in specific heat that manifest the fractal structure of the Hofstadter butterfly. We also propose experimental approaches which use specific heat as an access to detect the Hofstadter butterfly.

KEYWORDS: Hofstadter model, quantum transfer matrix method, specific heat oscillation

1. Introduction

The interplay between crystalline potential and magnetic field on a two-dimensional electronic gas remains a nontrivial problem for decades.¹⁾ This issue provides a stage on which purely mathematical concepts, i.e., the irrationality of a real number, interrupts our intuition of physical reality. Hofstadter²⁾ studied the energy spectrum of the tight-binding limit of this problem, namely, the Hofstadter model. He proposed a fractal topology for the spectrum (Hofstadter butterfly), which reconciled the paradox raised by the irrationality. The experimental verification of the Hofstadter butterfly is challenging but some hints of the fractal structure have been observed in microwave measurements,^{3,4)} Hall conductivity⁵⁾ and magnetic transport measurements⁶⁾ in analogous systems. The effects from the disorder and anisotropy are discussed in ref. 7.

In this paper, we adopt a recently developed quantum transfer matrix method⁸⁾ to study thermodynamic properties of the Hofstadter model. We focus on the behavior of internal energy and specific heat as functions of magnetic field. As far as we know, this is the first report that by theoretical method, the fractal structure in the Hofstadter butterfly can be studied by computing the specific heat in a magnetic field of a generic value. We also briefly discuss the feasibility of experimental observations of these features.

In a previous publication,⁹⁾ we had used the quantum transfer matrix method to study the magnetic properties of Hofstadter model. The advantage of this method lies in that it directly computes the partition function of the model for arbitrary ϕ , where ϕ is the magnetic flux through a unit cell, then the thermodynamic properties can be studied steadily. Conventional theoretical methods, such as Bethe ansatz^{10,11)} and exact diagonalization,^{12,13)} are mostly applied to $\phi = p/q$ cases, where p and q are mutually prime numbers, and q is relatively small. Although detailed information of energy spectrum and wavefunction can be obtained with these methods, only limited cases of ϕ can be studied and most discussion was focused on ground state properties. Besides, at ground states, due to the fractality of the Hofstadter butterfly, the smoothness of physical quantities as functions of magnetic field, such as total energy, static

magnetic susceptibility are significantly diminished. However, within the quantum transfer matrix formulation, the effect of finite temperature is embodied in the partition function at the beginning, and the singularities due to the fine fractality will be smeared out and the smoothness of physical quantities can be recovered, which makes the comparison to experimental results more straightforward.

2. Model and Method

Hofstadter model describes the dynamics of two-dimensional tight binding electrons in a uniform magnetic field.²⁾ By applying Landau gauge, i.e., $A = H(0, x, 0)$, the Hamiltonian is explicitly translationally invariant along the y -direction. Fourier transformation along the y -axis will then decouple the two-dimensional model H into a series summation of one-dimensional Hamiltonian H_k :

$$H = \sum_k H_k, \quad (1)$$

$$H_k = \sum_x [tc_{k,x+1}^\dagger c_{k,x} + tc_{k,x}^\dagger c_{k,x+1} + 2t \cos(2\pi x\phi - k)c_{k,x}^\dagger c_{k,x}], \quad (2)$$

where $k = 2\pi n/N_y$ ($n = 0, 1, \dots, N_y - 1$) are the quasimomenta and N_y is the lattice dimension along y direction. x is the lattice coordinate of electrons along the x -axis. ϕ is the magnetic flux through each plaquette, with magnetic flux quanta hc/e as unit.

H_k does not generally have translational invariance along the x -axis. But for rational $\phi = p/q$, periodicity can be recovered by combining every q cells to form a superlattice, and then the problem can be solved by diagonalizing a $q \times q$ matrix for each quasimomentum of the superlattice. Thus the full energy spectrum and thermodynamic properties can be steadily obtained, yet apparently, only up to relatively small q . To study cases with a generic ϕ , the quantum transfer matrix method starts from the partition function $Z = \text{Tr}[\exp(-\beta H)]$, which can be viewed as an trace of the evolution operator along the imaginary time. Since the trace naturally imposes a periodical boundary condition, a Fourier transformation can be well defined along the imaginary time (the inverse temperature), which is the key point leading us to the transfer matrix representation and to significantly simplify the calculation in refs. 8 and 9. Given k , the partition function of H_k is defined by

*E-mail: liping0710@gmail.com

$$Z_k = \text{Tr} \exp(-\beta H_k), \quad (3)$$

where $\beta = 1/k_B T$. The partition function of the whole system is simply a product of all Z_k s. By making use of the translational invariance along the imaginary time, Z_k can be expressed as a product of N_x 2×2 matrices. After multiplying different k components, we can obtain the partition function of the system, from which one can calculate the free energy by $F = -(1/\beta) \ln Z$, and other thermodynamic quantities such as magnetic susceptibility and specific heat.

In ref. 9, the authors have discussed the effect of lattice size on the numerical results. Accordingly, we choose here $N_x = 50000$ and $N_y = 100$ to ensure the numerical accuracy as well as computational efficiency for the temperature range in this paper. For simplicity, we only consider the half-filling case, which corresponds to a particle-hole symmetry and automatically sets chemical potential μ to 0. The chemical potential oscillation with the flux quanta and the related impact on magnetization oscillation were discussed in ref. 14.

3. Results and Discussion

First, we calculate the average internal energy as a function of ϕ at $T = 0.01$.

As shown in Fig. 1, at the local minima of the internal energy, the electron count ν ($= 0.5$ for half-filling) and ϕ satisfy the relation in eq. (4), which was given ref. 12. These minima are *cusp*-like.

$$\nu = M + N\phi, \quad M, N \in \mathbb{Z}. \quad (4)$$

The global minimum in Fig. 1 is consistent with the conclusion that there is an global minimum of the average energy^{13,15} when $\phi = \nu = 1/2$, that is, each electron carries one flux quanta. We have marked the values of ϕ (the red number on the top axis) located at distinguishable minima and the corresponding integers M and N in Fig. 1. At zero temperature, the average energy will not be smooth almost everywhere because there are infinite number of rational ϕ s that satisfy eq. (4). But here the temperature will erase minor singularities and only keep the significant ones.

Then we compute the specific heat from the first order derivative of the internal energy with respect to the temperature. Figure 2 shows the specific heat C as a function of temperature T for some special ϕ s. The chosen three ϕ s belong to the pure cases in Hofstadter's proposal,² i.e., $\phi = 1/N$, or $1 - 1/N$ when $N \geq 2$. Under magnetic field of these values, the single Bloch band in zero magnetic field is split into N subbands. If N is odd, the central subband has a van-Hove singularity at the center point of the energy spectrum ($E = 0$). If N is even, the density of states (DOS) goes to zero at $E = 0$.¹² When the temperature is so high that the thermal fluctuations are comparable to the energy difference between the lowest and the highest subband, the subbands will not be able to manifest their internal fine structures from specific heat. This can be observed from the high temperature tail in Fig. 2.

The difference in the specific heat for various values of ϕ will emerge with the decreasing temperature. First, at low temperature, the behavior of specific heat can tell the singularity of DOS at the energy spectrum center point [the Fermi surface (FS) in our half-filling case]. In the regime

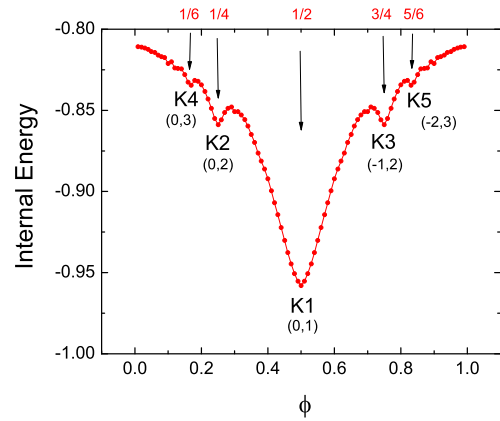


Fig. 1. (Color online) The internal energy as a function of ϕ for the Hofstadter model at half filling. $T = 0.01$. Some values of ϕ (the red number above the top axis) and the integers (M, N) corresponding to local minima are marked.

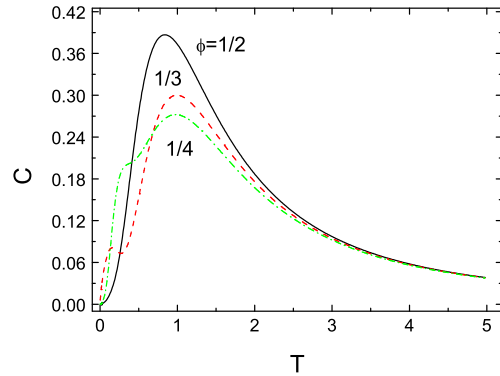


Fig. 2. (Color online) Temperature dependence of the specific heat C at half filling for $\phi = 1/2, 1/3, 1/4$.

near zero temperature, the $\phi = 1/2$ and $1/4$ curves are decreasing faster than that of $\phi = 1/3$. A closer observation indicates that the specific heat coefficient C/T in the case of $\phi = 1/2$ and $1/4$ decrease linear-like, while $\phi = 1/3$ diverges, with the temperature decreasing. This is because of the different behavior of DOS at the spectrum center point.¹² For $\phi = 1/2$ and $1/4$, the original single band in zero field splits up into 2 and 4 bands. But the centermost two bands are not completely separated by a gap, rather they “kiss” at the center point, where DOS of both bands linearly goes to zero. For $\phi = 1/3$, the Bloch band splits into three bands, and DOS of the center band is singular at the center point, which corresponds to the divergence of C/T when approaching zero temperature.

In the intermediate temperature regime, the specific heat tells the information about gaps and redistribution of DOS along the energy spectrum. In Fig. 2, the curves of $\phi = 1/3, 1/4$ show some similar minor hump structures, which is different from the case of $\phi = 1/2$. For $\phi = 1/2$, two subbands touch at FS, where DOS is zero, and there is no finite gap in the energy spectrum. Thus there is only one major hump in specific heat curve. For both $\phi = 1/3$ and $1/4$, there is a finite gap lying above FS,¹² which separates the subband on ($\phi = 1/3$) or near ($\phi = 1/4$) FS from the higher band, and gives the extra minor hump in the specific heat curve.

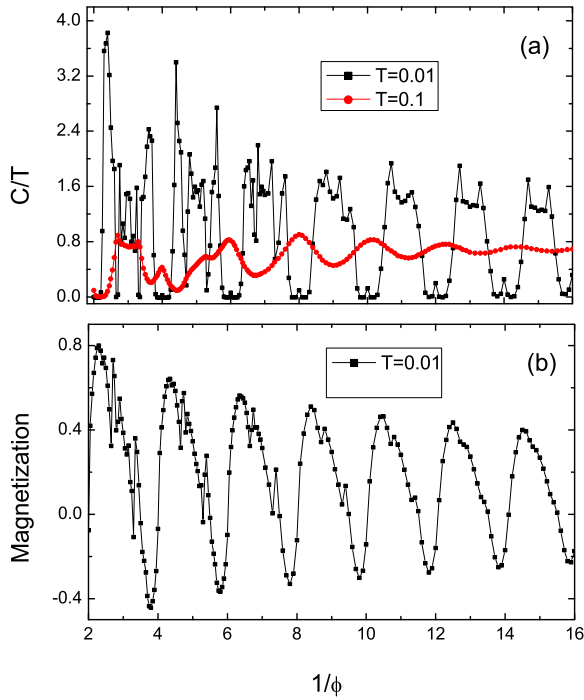


Fig. 3. (Color online) (a) The specific heat coefficient C/T as a function of $1/\phi$. Two different temperatures $T = 0.01, 0.1$ are compared. (b) Magnetization at $T = 0.01$ as a function of $1/\phi$.

Figure 3(a) shows the specific heat coefficient (C/T) as a function of magnetic field at different temperatures, $T = 0.1$ and 0.01 . The horizontal axis is chosen as $1/\phi$, so that the conventional de Haas–van Alphen (dHvA)-like oscillations are shown distinctly in the figure. The period $\Delta(1/\phi)$ of this oscillation is about 2 in both cases, which is consistent with that obtained from textbook formula,¹⁶⁾ $\Delta(1/\phi) = 4\pi^2/S_F$, where S_F is the Fermi volume. At half filling, $S_F = 2\pi^2$, thus $\Delta(1/\phi) = 2$ in Fig. 3(a).

However, a more important observation is that subtle oscillations emerge within the dHvA-type period with decreasing temperature and strong field. The specific heat at $T = 0.1$ displays a clean periodic oscillation on the weaker field side (large $1/\phi$), while this periodicity is disturbed in the stronger field regime (small $1/\phi$). This becomes more explicit with lower temperature $T = 0.01$. In the first three periods, very sharp peaks and dips show up, and they make a peculiar type of oscillations within the period. Even for weaker field regime, some sharp structures are still observable. It is worthwhile to note that the locations of the maximums (or minimums) for the cases in $T = 0.1$ and 0.01 do not match, which is just the representation of the energy resolution scale. The higher the energy resolution, the more gaps and the finer structure can be detected. Here, the lower temperature is the finer measurement for the fractal energy spectrum. Those gaps distinguished by the temperature $T = 0.01$ are beyond the detection regime of $T = 0.1$. As a consequence, those minimums shown in the case of $T = 0.01$ become the maximums due to the average on the larger energy intervals in the case of $T = 0.1$.

For the purpose of comparison, Fig. 3(b) shows the magnetization oscillation with respect to the magnetic field. Similar to the specific heat, the main envelope of oscillation

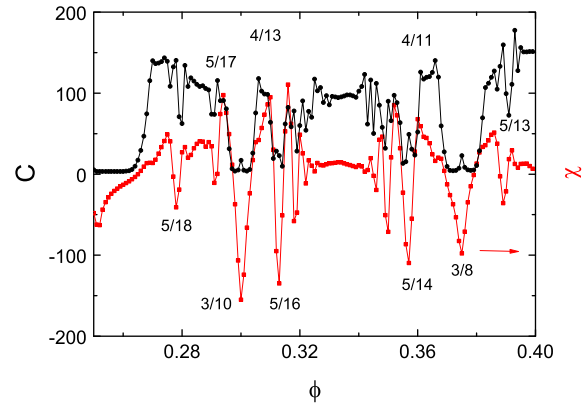


Fig. 4. (Color online) Specific heat coefficient (black line) and magnetic susceptibility (red line) for the Hofstadter model at half-filling. The numerical values of specific heat are 6000 times larger than the original ones for comparison. The values of ϕ s marked corresponds to some local maxima and minima in both specific heat and magnetic susceptibility.

is the conventional dHvA oscillation. Besides, subtle structures emerge within the dHvA period.⁹⁾ By comparing the results for magnetization and specific heat, we find that the specific heat oscillations are more distinct and drastic.

To explore the information about the fractal structure of Hofstadter butterfly from specific heat, we zoom in the first period in Fig. 3 and then have Fig. 4 for low temperature specific heat C and magnetic susceptibility χ . The numerical values of the specific heat are enlarged to 6000 times of the original values for a clear comparison. Here ϕ is chosen to be the horizontal axis. The consistency between C and χ is obvious if we compare the positions of local maxima and minima of both quantities. In Fig. 4 some fractional values of ϕ s are marked where they are close to the local maxima and minima. Applying Hofstadter’s proposal of constructing the butterfly,²⁾ we can extract the structure of energy spectrum at these ϕ s and understand why the extrema of C and χ are close to them. With Hofstadter’s proposal, each fractional ϕ can be decomposed to a set of more “fundamental” fractions, or, “local variable” as in ref. 2, which then directly displays the splitting of subbands in the energy spectrum. For example, for $\phi = 4/13$, the center local variable is $4/5$, which means there is a cluster of 5 subbands centered at FS. Consequently, a van-Hove singularity of DOS shows up at FS and causes the local maximum in C and the strong paramagnetism (local maximum in χ),⁹⁾ while for $\phi = 3/8$, the center local variable is $1/2$, thus there are two subbands lying above and below FS with a zero DOS at FS and consequently in Fig. 4, C shows a small value (close to 0) around $\phi = 3/8$ and χ is strongly diamagnetic around $\phi = 3/8$.

Therefore, by decreasing the temperature, fractal structures of the Hofstadter butterfly manifest themselves by producing peculiar oscillatory features within conventional dHvA period. This emergence along with decreasing temperature is due to the fact that temperature provides the only energy scale that sets up the resolution of the spectrum. Temperature erases minor bands and gaps that are smaller than the scale of temperature and restores the smoothness of physical quantities. But fractal structures with an energy scale larger than the temperature survive, and are able to

manifest themselves by displaying smoothened singularities in thermodynamic quantities. Thus the subtler fractal structures of Hofstadter butterfly can be probed by the measurement of the specific heat at lower temperatures.

Hall conductance oscillation^{5,17,18} have opened the detection window for the special band structure. Here, from the perspective of measurement for the thermodynamic quantity, we propose to adopt the superconducting thin films (for example the element Nb) with periodic arrays of pinning sites¹⁹ to realize this temperature-dependent emergence of fractal structures in specific heat. The artificial pinning centers hold great potential. Just below the onset temperature of superconducting transition, the electrons possess long mean free path. When the interval between adjacent sites comes to the order of 100 nm, the experimentally accessible steady fields can enter the interesting regime of ϕ . The resulting effective lattice subjected to perpendicular magnetic field is probably able to show the fractal properties of the Hofstadter model. In addition, the purity requirement of the sample is relaxed when considering the specific heat measurement.

4. Conclusion

In summary, adopting the quantum transfer matrix method, we compute the internal energy and specific heat of the Hofstadter model, and for the first time we study the oscillation of the specific heat with varying magnetic field as a signature of fractal structure of the Hofstadter butterfly. In low field regime, the oscillation period of specific heat is consistent with the conventional dHvA oscillation. When the temperature is decreased, sharp peaks and dips emerge in addition to the dHvA-type background. These peculiar oscillatory behaviors are direct indications of DOS in the fractal energy spectrum. We also suggest the possibility of

making use of superconducting films to detect this fractal structure by measuring the specific heat.

Acknowledgments

We thank Shao-Jing Qin for helpful discussions. Li-Ping Yang acknowledges generous hospitality of Xiao Hu during her visit in Japan. This work was supported by the Dutch Science Foundation (FOM) and the NSF-China.

-
- 1) P. G. Harper: *Proc. Phys. Soc. London, Sect. A* **68** (1955) 874.
 - 2) D. R. Hofstadter: *Phys. Rev. B* **14** (1976) 2239.
 - 3) U. Kuhl and H.-J. Stöckmann: *Phys. Rev. B* **80** (1998) 3232.
 - 4) R. R. Gerhardt, D. Weiss, and U. Wulf: *Phys. Rev. B* **43** (1991) 5192.
 - 5) C. Albrecht, J. H. Smet, K. v. Klitzing, D. Weiss, V. Umansky, and H. Schweizer: *Phys. Rev. Lett.* **86** (2001) 147.
 - 6) R. R. Gerhardt, D. Weiss, and K. v. Klitzing: *Phys. Rev. Lett.* **62** (1989) 1173.
 - 7) M. Koshino and T. Ando: *J. Phys. Soc. Jpn.* **73** (2004) 3243.
 - 8) L. P. Yang, Y. J. Wang, W. H. Xu, M. P. Qin, and T. Xiang: *J. Phys.: Condens. Matter* **21** (2009) 145407.
 - 9) W. H. Xu, L. P. Yang, M. P. Qin, and T. Xiang: *Phys. Rev. B* **78** (2008) 241102.
 - 10) P. B. Wiegmann and A. V. Zabrodin: *Phys. Rev. Lett.* **72** (1994) 1890.
 - 11) Y. Hatsugai, M. Kohmoto, and Y. S. Wu: *Phys. Rev. Lett.* **73** (1994) 1134.
 - 12) Y. Hasegawa, P. Lederer, T. M. Rice, and P. B. Wiegmann: *Phys. Rev. Lett.* **63** (1989) 907.
 - 13) G. Montambaux: *Phys. Rev. Lett.* **63** (1989) 1657.
 - 14) V. M. Gvozdkov and M. Taut: *Phys. Rev. B* **75** (2007) 155436.
 - 15) P. G. Harper: *Phys. Rev. B* **41** (1990) 9174.
 - 16) N. W. Ashcroft and N. D. Mermin: *Solid State Physics* (Thomson Learning, New York, 1976).
 - 17) V. M. Gvozdkov and M. Taut: *New J. Phys.* **11** (2009) 063005.
 - 18) M. C. Geisler, J. H. Smet, V. Umansky, K. v. Klitzing, B. Naundorf, R. Ketzmerick, and H. Schweizer: *Phys. Rev. Lett.* **92** (2004) 256801.
 - 19) K. Harada, O. Kamimura, H. Kasai, T. Matsuda, A. Tonomura, and V. V. Moshchalkov: *Science* **274** (1996) 1167.